Patterns of Detonation Decay and Combustion of Hydrogen-Air Mixture in Porous Layer

Sergey V. Golovastov, Grigory Yu. Bivol
Joint Institute for High Temperatures of Russian Academy of Science
125412, Moscow, Russia. Izhorskaya str., 13, build. 2

1 Introduction

Hydrogen is considered as a promising environmentally friendly fuel. However, the use of hydrogen is associated with a high probability of spontaneous explosions and structural damage. On the one hand, it is a gas capable of escaping from the room in a short time. On the other hand, the molecular-kinetic properties of hydrogen allow it to ignite over the widest concentration range with minimum ignition delay. In those cases where the presence of a ventilation system and an active safety system may not be sufficient to prevent ignition or quenching in enclosed spaces, passive safety systems that prevent the formation of detonation of hydrogen-air or hydrogen-oxygen mixtures must be developed. The most urgent task is to ensure safety from explosion at nuclear facilities, where forced ventilation of process rooms has significant limitations. As an example of the passive safety system a porous coating on internal walls can be used.

Considering the problem of reducing the shock-wave effect on a structural material, the motion of a shock wave and the mass of compressed gas directed along the normal direction to the surface under investigation is often studied [1]. The porous wall effect on detonation propagation was considered in [2,3]. It was shown in [4] that the influence of non-reflecting walls leads to a considerable reduction in the existence domain for the near-limit detonation regimes. Since the front of the detonation wave has a cellular structure formed by the motion of transverse waves, the presence of a porous coating leads to a weakening of the intensity of these waves, and to a decrease in the intensity of the detonation wave and to its decay [5-7]. Subsequently, various devices to suppress detonation were compared in [8-10]. The experiments show that materials with a porous structure (porolon, felt, sintepon) are the most efficient for quenching the transverse waves [11].

It is worth noting that in some cases the presence of a solid incompressible porous coating can lead to the acceleration of the flame front, and to the re-initiation of detonation [12]. The attenuation and re-initiation mechanism of detonations transmitted through a porous section was investigated experimentally and numerically in [13,14]. Attenuation and recovery of detonation wave after passing through acoustically absorbing section in a hydrogen-air mixture at atmospheric pressure was presented in [15].

Correspondence to: Sergey Golovastov golovastov@yandex.ru

The question of the evolution of the flame front during motion along the porous surface, during the decay of the detonation wave, remains poorly understood. The purpose of this work is to determine the patterns of the evolution of the flame front near the porous coating, as the force exerted by the shock wave and combustion products on the lateral surface of the detonation tube during tangential motion along the surface of the porous coating. The propagation of a detonation wave in the channel with a different pore size on the wall was experimentally examined.

2 Experimental set-up

Figure 1 shows the scheme of the experimental set-up. The set-up consisted of two sections: cylindrical section with length 2600 mm and inner diameter 20 mm; rectangular cross-section with length 500 mm and transverse dimensions 20×20 mm (solid walls) or 20×40 mm (porous walls).

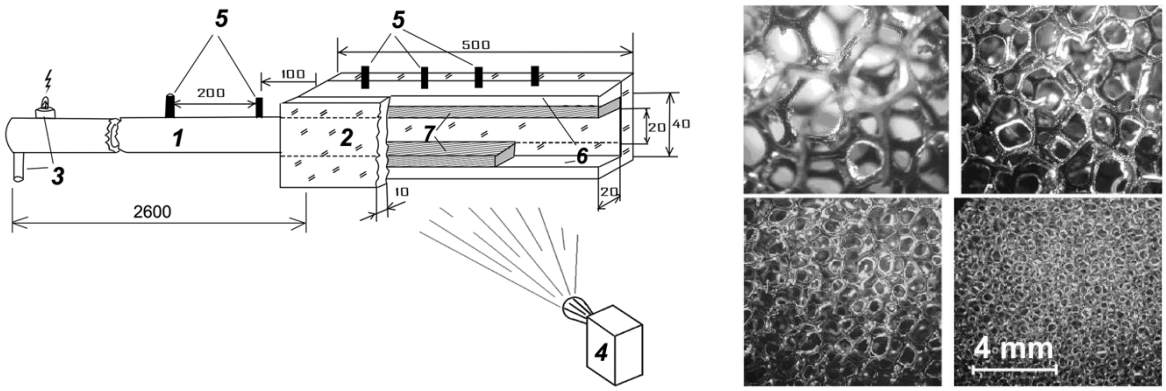

Figure 1. Left: scheme of experimental set-up; right: samples of the porous materials (10, 20, 40, 80 pores per inch). 1: detonation tube; 2: transparent rectangular section with acoustically adsorbing walls; 3: spark gap and supply of combustible mixture; 4: high-speed video camera; 5: pressure transducers (positions 60 mm, 160 mm, 260 mm and 360 mm); 6: solid walls; 7: porous walls (width 10 mm)

The methodology is described in detail in [16]. The transition from combustion to detonation was carried out in the cylindrical section of the detonation tube. The stationary detonation wave was formed before the second section. The entire inner surface of the section was covered with porous material. The layer thickness was selected so that the inner transverse dimension was 20 mm anywhere along the section. For visual observation of the flame front dynamics we used a rectangular section with transparent walls. To study the propagation of the detonation in the channel with solid walls, two steel plates were inserted into the channel so that the cross-sectional dimensions were equal to 20×20 mm. A number of pores per inch (PPI) was ranged from 10 to 80, as presented in the Figure 1.

To determine the pressure and velocity of the detonation wave four pressure transducers PCB (111A, 113B) were used. Inside the porous section transducers were mounted at 60 mm, 160 mm, 260 mm and 360 mm from the beginning of the section. For registration of the flame front, photodiodes FD-256 were installed, together with the pressure sensors. To observe the detonation wave front a high-speed digital camera Videosprint was used. In single-shot mode the frequency was equal to 6024–11494 Hz, 1 μs exposure, resolution 1280×100. The camera detects a radiation in the range 400–1000 nm.

3 Combustion inside the porous layer

Registration of the flame front within the rectangular channel using a Schlieren system was showed in details in [16]. In the case when the top and bottom walls of the rectangular channel are covered by the porous material with open pores, the camera recorded the deceleration of the flame front. In this case, the shape of the flame front undergoes changes. An Ω-shaped structure is formed, followed by a region of turbulent combustion. The most intense luminescence was observed at the boundaries of the adsorbing material with an open porous surface.

Combustion was also recorded inside the porous covering. A high-speed photographic recording was carried out using the external illumination of a 2-kW incandescent lamp. The use of the lamp with the indicated power allows exposure durations of 1 μs to avoid exposure from the luminous combustion products, and to detect the surface of the porous coating. Also, the use of an incandescent lamp of the indicated power allows, with an optimal choice of contrast, the determination of the boundaries of the zone of hot combustion products inside the porous coating.

The experiments were carried out for the two values of pores per inch: PPI 40 and PPI 20. Figure 2 shows the results of recording inside the porous coating and over its surface. The colors are inverted for Figure 2. The moment of time '0' is close to the moment of entry to the porous section.

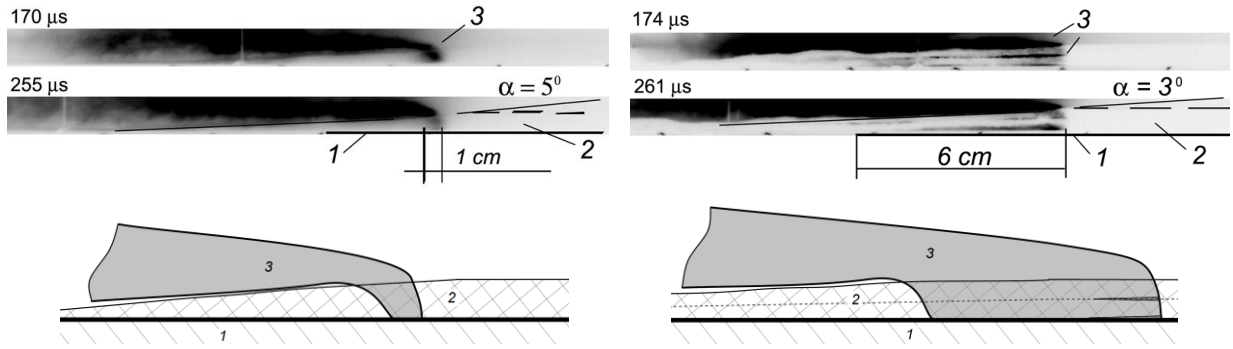

Figure 2. Serial frames of the flame front and combustion products and sketches for pores per inch PPI 40 (left) and PPI 20 (right).
1: solid walls; 2: porous layer, height 10 mm; 3: flame front, products of combustion. Colors are inverted

The dimensions of the combustion zone inside the porous coating are in direct proportion to the pore sizes. The smallest area of combustion is recorded for PPI 40. In this case, the longitudinal length of the combustion zone does not exceed the height of the coating 10 mm. For PPI 20 the length of the combustion zone is about 80 mm, and decreases to 60 mm. Increasing the size of pores obviously leads to an increase in heat transfer between the layers of the gas mixture. In addition, increasing the pores results in the longitudinal expansion of the combustion products inside the layer with less resistance.

The strip-like combustion zone shown in Fig. 2 (right) for PPI 20 can be explained by the fact that the composite layer of porous polyurethane was used, consisting of two plates with a thickness of 5 mm each, 10 mm in total. This allows to vary the thickness of the layer. Therefore, at the place of the joints of the layers and near the metal surface, the burning area looks brighter (the dark area in the color inverted frames). These areas are highlighted in the sketch.

Deceleration of combustion products with increasing relative distance behind the flame front leads to an increase in the static pressure exerted on the side surface of the porous coating. In this case, compression of the porous coating immediately after passing through the flame front is recorded. Moreover, with the increase in the above distance to the flame front, the compression ratio increases. The presence of porosity with the simultaneous compression of foam rubber leads to the fact that the combustion products expand, mainly in the transverse direction, flowing into the core of the flow. In this case, this probably involves the displacement of hot combustion products from the porous layer.

It should be expected that an increase in the pore size results, to a lesser extent, in the displacement of the combustion products. The static pressure over the larger pores is lower than over the smaller pores. This results in less compression of the porous coating. For example, it can be seen from the Figure 2 that the angle formed between the surface of the porous coating and the channel axis takes on a larger value for smaller pores. For PPI 40 it is equal to 5°, and for PPI 20 this angle is equal to 3°.

4 Parameters of shock wave under the porous layer

Typical oscillograms of pressure under different kinds of porous layer can be find in [16]. On the based of these oscillograms pressure evolutions for porous materials with different pore sizes were determined and presented in Figure 3. The pressure at the first sensor was in the range from 1.0 to 1.4 MPa for all porous materials, with the highest pressure (1.4 MPa) recorded while using PPI 10. The final pressure showed a direct dependence of the pressure on the wall on the pore size: the lowest pressure (about 0.6 MPa) was observed when using PPI 40 and PPI 80, the highest when the case of PPI 40 and PPI 80, a monotonic pressure drop was observed, while in larger types of polyurethane foam a pressure minimum at the distance of 160 mm from the beginning of the porous section is observed, followed by a pressure increase.

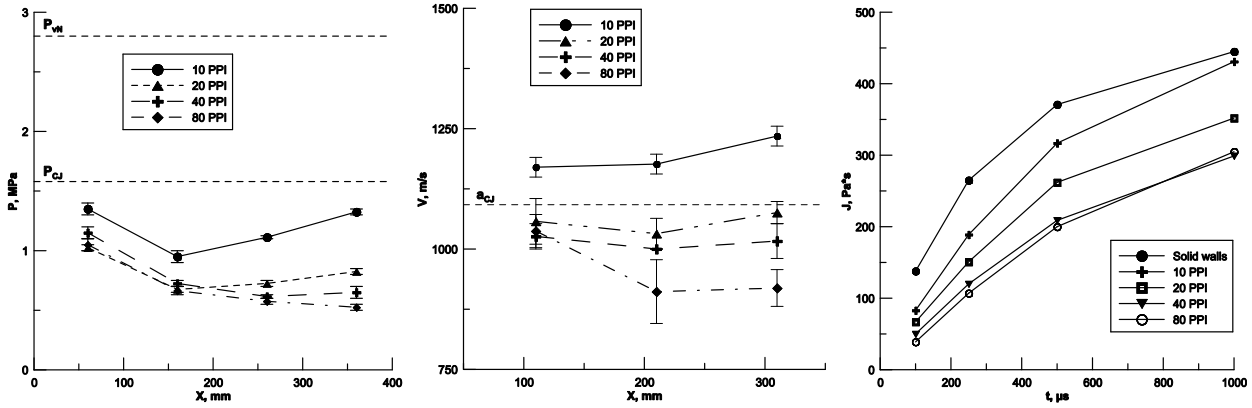

Figure 3. Evolution of the shock wave pressure *P* (left), shock wave velocity *V* (centre) and pressure impulse *J* (right) in the porous section for different values of PPI

The evolution of the velocity of the shock wave is shown in Figure 3. Similarly to the pressure dependence on the pore size, the highest wave velocity was observed in PPI 10. The initial velocity was 1150 m/s, the final velocity was 1250 m/s. As the pore size decreases, the wave propagation velocity also decreases: for the PPI 80, the final speed is 900 m/s, which is less than half of the Chapman-Jouguet detonation velocity (1950 m/s). Similarly to the amplitude of the shock wave, in the case of PPI 10 and PPI 20, the increase in propagation velocity of the wave after the initial decrease is observed. In PPI 40 and PPI 80 shock wave

velocity decreases monotonically. We can see that the shock wave velocity in case of PPI 10 is higher, than Chapman–Jouguet sound velocity.

Pressure impulse, which is a pressure integral over time, was calculated using pressure readings:

$$J = \int_0^{\tau} P dt \tag{1}$$

Figure 3 presents the values of the pressure impulse on the last sensor #4 (position 360 mm) for the intervals τ of 100, 250, 500 and 1000 μs after the arrival of the shock wave. From the graph it can be seen that the pressure impulse per 100 μs is about 140 Pa*s for the case of a solid wall. When using PPI 80 and PPI 40 the impulse decreases to 40-50 Pa*s and for PPI 10 and PPI 20 the impulse decreases to 40-50 Pa*s. Overall the impulse decreases when using porous material with small and big pores by 3 and 2 times, respectively. With an increase in the integration time, the difference is diminished, for 1000 μs the impulse is 440 Pa*s for a solid channel, 425 Pa*s for a channel with PPI 10 and 300 Pa*s for PPI 80. For all the integration intervals used, the shock wave impulse in the solid channel remained higher than when using the polyurethane foam on the wall. However the pressure impulse for PPI 10 increases significantly almost reaching the values in the case of solid channel. It means that the effect of porous material with big pores is similar to solid walls. Further increasing the integration time the pressure impulse values should become stationary.

5 Conclusions

The processes of decay of the detonation wave in hydrogen-air mixture during propagation along a porous surface were considered. As a porous coating, polyurethane porous coatings were used with pores per inch (PPI) varied from 10 to 80. The presence of the porous coating leads to the decay of the detonation wave into a shock wave and the flame front following it.

A non-monotonic influence of the parameters of the porous coating on the evolution of the detonation wave in the channel was observed. When a porous material with large pores (10 and 20 pores per inch) is used, the pressure and wave velocity decrease first, after which the pressure and velocity of the wave increase over a distance of more than 300 mm from the beginning of the porous section. When the wave propagates in a polyurethane foam with small pores (40 and 80 pores per inch). The final pressure in PPI 10 is twice as high as in PPI 80, and the final velocity is 40% higher in PPI 10 than in PPI 80. Such a large difference in the parameters of the detonation wave can be explained by the weakening of the transverse waves in PPI 40 and PPI 80, while in PPI 10 and PPI 20 the transverse waves pass through the porous material without attenuation, are reflected from the solid wall and support detonation combustion in the channel.

6 Acknowledgements

The work was supported by the Program of Fundamental Support of Academic Institutes.

References

[1] Gubaidullin AA, Britan A, Dudko DN. (2003). Air shock wave interaction with an obstacle covered by porous material. Shock Waves 13: 41.

[2] Evans MW, Given FI, Richeson Jr WE. (1955). Effects of attenuating materials on detonation induction distances in gases. J. Appl. Phys. 26: 1111.

[3] Zhang B. (2016). The influence of wall roughness on detonation limits in hydrogen–oxygen mixture. Combust. Flame 169: 333.

[4] Sharypov OV, Pirogov YA. (1995). On the mechanism of weakening and breaking of gas detonation in channels with acoustically absorbing walls. Comb. Expl. Shock Waves 31: 466.

[5] Dupre G, Peraldi O, Lee JH, Knystautas R. (1988). Propagation of detonation waves in an acoustic absorbing walled tube. Prog. Astronaut. Aeron. 114: 248.

[6] Radulescu MI, Lee, JH. (2002). The failure mechanism of gaseous detonations: experiments in porous wall tubes. Combust. Flame 131: 29.

[7] Mehrjoo N, Gao Y, Kiyanda CB, Ng HD, Lee JH. (2015). Effects of porous walled tubes on detonation transmission into unconfined space. Proc. Combust. Inst. 35: 1981.

[8] Guo C, Thomas G, Li J, Zhang D. (2002). Experimental study of gaseous detonation propagation over acoustically absorbing walls. Shock Waves 11: 353.

[9] Xie Q, Wen H, Ren Z, Liu H, Wang B, Wolanski P. (2017). Effects of silicone rubber and aerogel blanket-walled tubes on H2/Air gaseous detonation. J. Loss Prev. Process Ind. 49: 753.

[10] Yan XQ, Yu JL. (2013). Effect of aluminum silicate wool on the flame speed and explosion overpressure in a pipeline. Comb. Expl. Shock Waves 49: 153.

[11] Vasil'ev AA. (1994). Near-limiting detonation in channels with porous walls. Comb. Expl. Shock Waves 30: 101.

[12] Johansen C, Ciccarelli G. (2008). Combustion in a horizontal channel partially filled with a porous media. Shock Waves 18: 97.

[13] Radulescu MI, Maxwell BM. (2011). The mechanism of detonation attenuation by a porous medium and its subsequent re-initiation. J. Fluid Mech. 667: 96.

[14] Qin H, Lee JH, Wang Z, Zhuang F. (2015). An experimental study on the onset processes of detonation waves downstream of a perforated plate. Proc. Combust. Inst. 35: 973.

[15] Bivol GY, Golovastov SV, Golub VV. (2016). Attenuation and recovery of detonation wave after passing through acoustically absorbing section in hydrogen-air mixture at atmospheric pressure. J. Loss Prev. Process Ind. 43: 311.

[16] Golovastov SV, Bivol GY, Alexandrova D. (2019). Evolution of detonation wave and parameters of its attenuation when passing along a porous coating. Exp. Therm. Fluid Sci. 100: 124.